

Tunable Single Bandpass Microwave Photonic Filter With an Improved Dynamic Range

Xiuyou Han, *Member, IEEE*, Enming Xu, and Jianping Yao, *Fellow, IEEE*

Abstract—A tunable single bandpass microwave photonic filter (MPF) with an improved spurious free dynamic range (SFDR) using a dual-parallel Mach-Zehnder modulator (DP-MZM) and a phase-shifted fiber Bragg grating (PS-FBG) is proposed and experimentally demonstrated. The DP-MZM is employed to generate an equivalent phase-modulated (EPM) signal with an adjustable optical carrier to sideband ratio. The PS-FBG is used as an optical notch filter to remove one sideband of the EPM signal to convert the EPM signal to a single-sideband intensity-modulated signal. At the output of a photodetector, a microwave signal is detected. The entire operation is equivalent to a single passband MPF. The tunability is achieved by tuning the wavelength the optical carrier. The SFDR of the MPF is improved due to the gain enhancement by a partial suppression of the optical carrier. An experiment is performed. A single bandpass MPF with a passband width of 150 MHz and a frequency-tunable range of ~ 5.5 GHz with an improved SFDR by 11 dB is demonstrated.

Index Terms—Microwave photonic filter, single bandpass filter, dynamic range.

I. INTRODUCTION

MICROWAVE photonic filters (MPFs) have been intensively investigated in the past few years thanks to the key advantages such as wide tunable range, flexible tunability and good reconfigurability [1]–[3]. Among the different types of MPFs, single bandpass MPFs are one of the most important types of MPFs which can find applications in modern radar, communications, and warfare systems. Usually, a delay-line MPF with discrete time delays has a spectral response that is periodic (the period is equal to the free spectral range) [4]. To achieve an MPF with a single passband, one may use a broadband optical source sliced by a Mach-Zehnder interferometer (MZI) [5]. Due to the continuous nature of the optical spectrum, an MPF with a single passband can

be realized. However, the noise figure of the MPF is very large and the dynamic range is small due to the strong relative intensity noise (RIN) of the broadband optical source. On the other hand, a single bandpass MPF can be implemented in the coherent regime using a phase modulator (PM) and an ultra-narrow optical notch filter, where a tunable laser source (TLS) with a low RIN is utilized. By using the notch of the optical notch filter to remove one sideband of the phase-modulated signal, the phase-modulated signal is converted to a single-sideband (SSB) intensity-modulated signal. At the output of a photodetector (PD), a microwave signal is detected. The entire operation is equivalent to a single passband MPF with the center frequency tunable by tuning the wavelength of the optical carrier. The optical notch filter can be a ring resonator [6] or a phase-shifted fiber Bragg grating (PS-FBG) [7]. Although a TLS is used in the MPF, the spurious free dynamic range (SFDR) is still limited due to the low gain of the MPF. In [8] we demonstrated a single bandpass MPF with an improved dynamic range using a stimulated Brillouin scattering (SBS)-assisted adaptive filter. By partially suppressing the optical carrier, the gain of the MPF is improved, which leads to the improvement of the SFDR. The major limitation of the approach in [8] is the large size. To trigger the SBS effect, a long fiber loop in the SBS-based optical filter is needed. In addition, the input optical power is also very high, which increases the complexity of the MPF.

In this letter, we propose and experimentally demonstrate a single bandpass MPF with an improved dynamic range using a dual-parallel Mach-Zehnder modulator (DP-MZM) and a PS-FBG. A DP-MZM has an MZI structure with two MZMs in the two arms and a phase shifter in the lower arm. The DP-MZM is utilized to generate an equivalent phase-modulated (EPM) signal with an adjustable optical carrier power by controlling the DC bias voltage applied to the internal MZM in the upper arm. The EPM signal with a partially suppressed optical carrier at the output of the DP-MZM is amplified by an erbium-doped fiber amplifier (EDFA) and sent to the PS-FBG via an optical circulator (OC), where one sideband of the EPM signal is removed and the EPM signal is converted to an SSB intensity-modulated signal. The operation is called phase-modulation to intensity-modulation (PM-IM) conversion. Upon detection at a photodetector (PD), a microwave signal is generated and the entire operation is equivalent to a single bandpass MPF with the central frequency of the passband determined by wavelength difference between the optical carrier and notch wavelength. Due to the partial suppression of the optical carrier, the carrier to sideband ratio (CSR) is decreased. If the

Manuscript received July 24, 2015; revised August 30, 2015; accepted September 11, 2015. Date of publication September 15, 2015; date of current version November 23, 2015. This work was supported by the Natural Sciences and Engineering Research Council of Canada. The work of X. Han was supported in part by the China Scholarship Council and in part by the Natural Science Foundation of Liaoning Province under Grant 201402002.

X. Han is with the Microwave Photonics Research Laboratory, School of Electrical Engineering and Computer Science, University of Ottawa, Ottawa, ON K1N 6N5, Canada, and also with the School of Physics and Optoelectronic Engineering, Dalian University of Technology, Dalian 116024, China.

E. Xu is with the Microwave Photonics Research Laboratory, School of Electrical Engineering and Computer Science, University of Ottawa, Ottawa, ON K1N 6N5, Canada, and also with the School of Optoelectronic Engineering, Nanjing University of Posts and Telecommunications, Nanjing 210046, China.

J. Yao is with the Microwave Photonics Research Laboratory, School of Electrical Engineering and Computer Science, University of Ottawa, Ottawa, ON K1N 6N5, Canada (e-mail: jpyao@eecs.uottawa.ca).

Color versions of one or more of the figures in this letter are available online at <http://ieeexplore.ieee.org>.

Digital Object Identifier 10.1109/LPT.2015.2478856

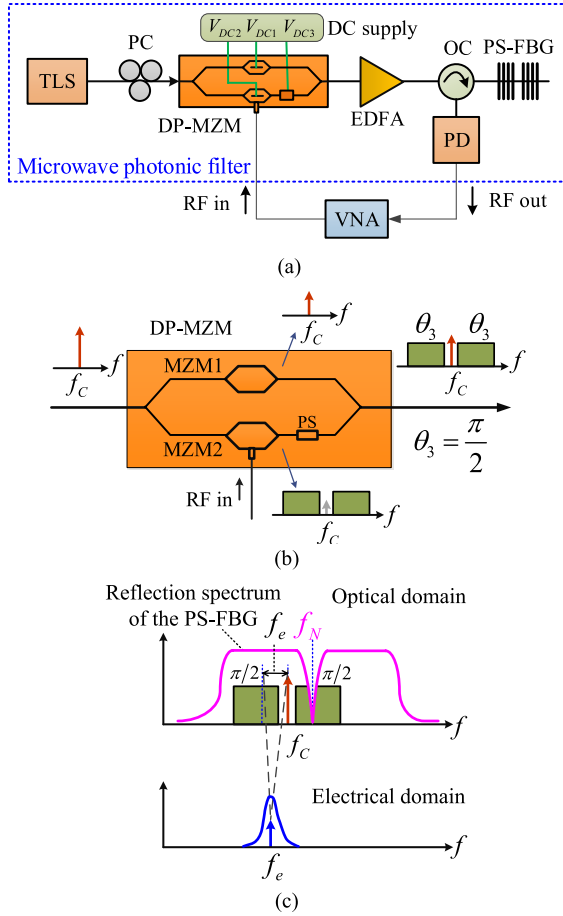


Fig. 1. (a) Schematic of the proposed MPF. (b) Principle to generate EPM signal with an adjustable optical carrier power. (c) Principle to achieve an MPF with a single bandpass. TLS, tunable laser source; PC, polarization controller; DP-MZM, dual-parallel Mach-Zehnder modulator; PS, phase shifter; EDFA, erbium-doped fiber amplifier; OC, optical circulator; PS-FBG, phase-shifted fiber Bragg grating; PD, photodetector; VNA, vector network analyzer.

optical power at the input of the PD is maintained unchanged by amplifying the EPM signal using the EDFA, the gain of the MPF is enhanced, which results in the improvement of the SFDR. An experiment is performed. A single bandpass MPF with a passband width of 150 MHz and a frequency-tunable range of about 5.5 GHz with an improved SFDR by 11 dB is demonstrated.

II. OPERATION PRINCIPLE

Figure 1(a) shows the schematic diagram of the proposed MPF. The spectral relationship between the optical carrier and the sidebands is shown in Fig. 1(b). As can be seen from Fig. 1(a), an optical carrier with a tunable frequency of f_c from a TLS is sent to a DP-MZM via a polarization controller (PC). The PC is used to align the polarization direction of the optical carrier with the principal axis of the DP-MZM to minimize the polarization-dependent loss. The DP-MZM, as shown in Fig. 1(b), consists of two sub-MZMs (MZM1 and MZM2) in the upper and the lower arms of the DP-MZM and a phase shifter (PS) also in the lower arm. For the upper arm, no microwave signal is applied to MZM1 and only a DC voltage V_{DC1} is applied, which is used to tune the output power of the optical carrier from MZM1.

For the lower arm, a microwave signal $V_e \cos(2\pi f_e t)$ from a vector network analyzer (VNA) with an amplitude of V_e and a frequency of f_e is applied to MZM2 to modulate the optical carrier. By controlling the DC bias voltage V_{DC2} , MZM2 is operating at the minimum transmission point to implement carrier-suppressed double-sideband (CS-DSB) modulation. The PS, to which a DC voltage V_{DC3} is applied, is used to generate a phase shift of θ_3 to the two sidebands of the CS-DSB signal. At the output of the DP-MZM, the optical signals from the two arms are combined. If the phase shift introduced by the PS is $\pi/2$, the optical signal at the output of the DP-MZM is equivalent to a phase-modulated signal, but with an adjusted carrier power or CSR. The optical signal at the output of the DP-MZM is amplified by an EDFA, and then sent to a PS-FBG. The PS-FBG has a narrow notch in the reflection band, which is used to remove one sideband. After photodetection at a PD, a microwave signal is generated which is sent back to the VNA to measure the frequency response of the MPF.

The electrical field of the optical signal from the DP-MZM can be expressed as [9]

$$E_1(t) = \frac{1}{2} E_0 e^{j2\pi f_c t} \cos \theta_1 + \frac{1}{4} E_0 e^{j2\pi f_c t} \left\{ \begin{array}{l} e^{j[m \cos(2\pi f_e t) + \theta_2]} \\ + e^{-j[m \cos(2\pi f_e t) + \theta_2]} \end{array} \right\} e^{j\theta_3} \quad (1)$$

where E_0 is the electrical field amplitude of the input optical carrier, $\theta_i = \pi V_{DCi} / V_{\pi i}$ ($i = 1, 2, 3$) is the phase shift generated by the DC bias voltage V_{DCi} , $V_{\pi i}$ is the half wave voltage of MZM1, MZM2, and the PS at DC; $m = \pi V_e / V_{\pi e}$ is the modulation index, and $V_{\pi e}$ is the half-wave voltage at the microwave frequency f_e . By the Jacobi-Anger expansion, (1) can be rewritten as

$$E_1(t) \approx \frac{1}{2} E_0 e^{j2\pi f_c t} \cos \theta_1 + \frac{1}{2} E_0 e^{j2\pi f_c t} \times \left[\begin{array}{l} J_0(m) \cos \theta_2 \\ - J_1(m) e^{-j2\pi f_e t} \sin \theta_2 \\ - J_1(m) e^{j2\pi f_e t} \sin \theta_2 \end{array} \right] e^{j\theta_3} \quad (2)$$

where J_0 , J_1 are the 0 and 1st-order Bessel function of the first kind. When deriving (2), only the 0- and ± 1 st-order components are considered. When MZM2 is biased to suppress the optical carrier, the phase shift θ_2 should be $\pi/2$. When the phase shift θ_3 is equal to $\pi/2$, (2) can be written as

$$E_1(t) = \frac{1}{2} E_0 \left[\begin{array}{l} \cos \theta_1 e^{j2\pi f_c t} - J_1(m) e^{j2\pi (f_c - f_e) t} e^{j\pi/2} \\ - J_1(m) e^{j2\pi (f_c + f_e) t} e^{j\pi/2} \end{array} \right] \quad (3)$$

As can be seen that the output signal has an expression that is equivalent to that of a phase-modulated signal [10] except that the amplitude of the optical carrier $J_0(m)$ is replaced by $\cos \theta_1$. Here, we call the signal an EPM signal. The power of the optical carrier can be easily adjusted by changing the DC bias voltage V_{DC1} applied to MZM1, while the powers of the two sidebands are maintained unchanged.

A phase-modulated signal will only generate a DC if directly detected at a PD due to the out of phase nature of the beat signals between the optical carrier and the two sidebands [10]. However, the PS-FBG in the MPF can be used to

remove one sideband (say, the +1st sideband, $f_c + f_e$), by locating the sideband in the narrow notch of the PS-FBG to achieve PM-IM conversion, as shown in Fig. 1(c). Because of the narrow notch of the PS-FBG, the removal of the sideband only occurs over a small frequency range. The entire operation is equivalent to a bandpass MPF with a central frequency equal to the frequency difference between the optical carrier and the notch of the PS-FBG. Therefore, the central frequency of the passband can be tuned by changing the wavelength of the optical carrier from the TLS.

In addition to the frequency tunability, an MPF is also required to have a large dynamic range. The dynamic range is characterized by its SFDR, which can be defined as the range of the power of an input signal over which the output fundamental signal is above the output noise floor and all spurious signals are less than or equal to the output noise floor [11]. When the 3rd-order distortion is considered, the SFDR is 2/3 of the distance between the noise floor and the output 3rd-order intercept point (OIP3). Thus, when the fundamental curve and the 3rd-order distortion curve, or equivalently the OIP3, are moving up by an amount, the SFDR would be increased by 2/3 of that amount.

In the proposed MPF, the CSR of the EPM signal can be flexibly tuned due to the independently controllable power of the optical carrier by controlling the DC bias voltage V_{DC1} . If there is no DC voltage applied to MZM1, the value of $|\cos\theta_1|$ is equal to 1 and the DP-MZM operates as a regular phase modulator. When a DC bias voltage V_{DC1} is applied to control the CSR to be 0 dB [12] while maintaining the optical power at the input of the PD unchanged, the gain of the MPF will be maximized. Since the gain is increased, at the output of the PD, the powers of the recovered fundamental and the 3rd-order distortions are correspondingly increased and the OIP3 is moved up. Therefore, the SFDR of the MPF is efficiently increased.

III. EXPERIMENT AND RESULTS

An experiment based on the configuration in Fig. 1(a) is performed. A light wave from the TLS (YOKOGAMA AQ2200) with a power of 10 dBm is sent to the DP-MZM (JDSU, 10 GHz) through the PC. The bias voltages from the DC power supply (KIKUSUI, 0.001 V) are tuned to control the DC bias voltages to MZM1, MZM2 and the PS. A microwave signal from the VNA (Agilent E8364A) is applied to MZM2 via the RF port. MZM2 is biased to operate in the CS-DSB state by controlling V_{DC2} . A phase shift of $\pi/2$ to the sidebands of the CS-DSB signal is generated via the PS by controlling V_{DC3} . The CSR of the EPM signal is tuned by controlling V_{DC1} applied to MZM1. After being amplified by the EDFA (Nortel, FA17UFAC), the EPM signal is sent to the PS-FBG via the OC and reflected to the PD (New Focus, 20 GHz). The output electrical signal from the PD is sent back to the VNA for frequency response measurement.

The two key devices in the proposed MPF are the DP-MZM and the PS-FBG. The DP-MZM is used to generate the EPM signal with an adjustable optical carrier power and the PS-FBG is used to implement PM-IM conversion. Fig. 2(a) shows the spectra of the EPM signal at the output of the DP-MZM with

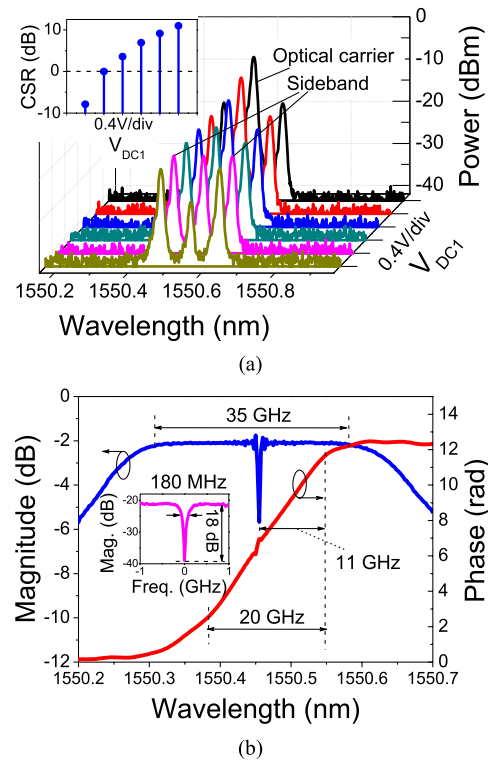


Fig. 2. (a) Optical spectra of the EPM signal at the output of the DP-MZM with different V_{DC1} . (b) The measured magnitude and phase responses of the PS-FBG.

different V_{DC1} applied to MZM1 when MZM2 is biased to operate in the CS-DSB state. It can be seen that the power of the optical carrier can be tuned by controlling V_{DC1} . As shown in the inset in Fig. 2(a), the CSR can be controlled to be 0 dB. Fig. 2(b) shows the magnitude and phase responses of the PS-FBG in reflection and a zoom-in view of the spectrum centered at the notch. The notch wavelength is 1550.455 nm, the 3-dB notch bandwidth is about 180 MHz, and the rejection ratio is about 18 dB. To implement PM-IM conversion, the two sidebands of the EPM signal should be within the linear phase response range of the PS-FBG to maintain their phase relationship [7]. The linear phase response range of the PS-FBG is about 20 GHz and is not fully symmetrical. The right section relative to the notch has a linear region of about 11 GHz, while left section relative to the notch has a linear region of about 9 GHz.

The tunability of the proposed single passband MPF is first investigated. The DC bias voltages to the DP-MZM are controlled to be $V_{DC2} = 5.10$ V to achieve CS-DSB modulation at MZM2, $V_{DC3} = 2.65$ V to achieve a phase shift of $\theta_3 = \pi/2$ at the PS, and $V_{DC1} = 0$ V to generate an EPM signal. The microwave signal from the VNA is swept from 0 to 5.5 GHz. The wavelength of the light wave from the TLS is tuned from 1550.460 to 1550.490 nm with a step of 0.005 nm. The measured frequency response of the MPF is shown in Fig. 3. As can be seen, the central frequency of the passband is tuned from 0.7 GHz to 4.56 GHz and the 3-dB bandwidth is about 150 MHz, and this value is maintained with negligible changes during the tuning process. This is another advantage of using this approach over a delay-line

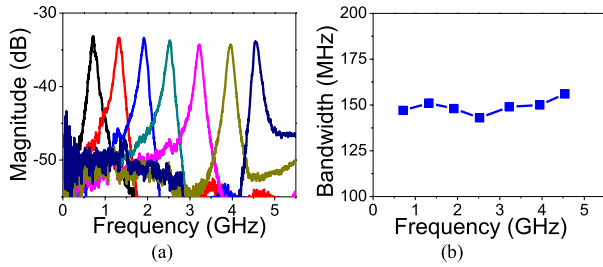


Fig. 3. Spectral response of the MPF. (a) Frequency tuning and (b) 3-dB bandwidth.

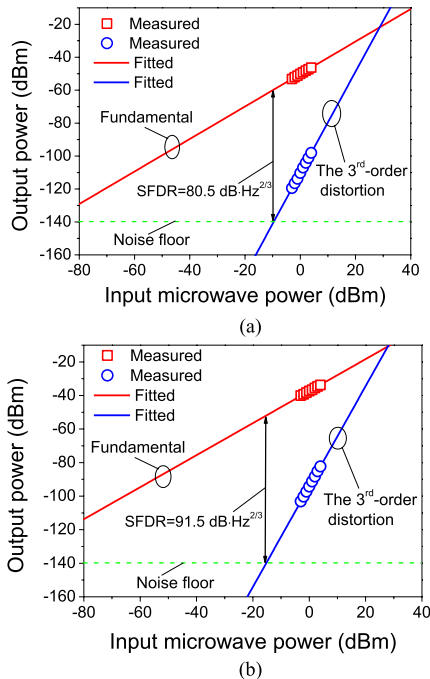


Fig. 4. The measured microwave powers of the fundamental and the IMD3 terms for (a) the optical carrier without suppression, and (b) the optical carrier partially suppressed with a CSR of 0 dB.

MPF where the tuning will usually change the shape of the spectral response.

Then, the improvement in the dynamic range is studied. To do so, we control the CSR of the generate EPM signal by tuning the DC bias voltage applied to MZM1. Two cases are studied here. First, the power of the optical carrier is controlled at its maximum value by letting $V_{DC1} = 0$ V. In this case, the DP-MZM is operating as a regular phase modulator. Then, the power of the optical carrier is controlled to make the CSR equal to 0 dB. For both cases, the optical power into the PD is fixed at 1 dBm which is achieved by controlling the gain of the EDFA. A two-tone microwave signal at 2.45 and 2.46 GHz is applied to the MPF. The output fundamental and the third-order intermodulation (IMD3) terms are measured when the power of the two-tone signal is increased from -3 to 4 dBm and the results are shown in Fig. 4. With no optical carrier suppression, the SFDR is measured to be $80.5 \text{ dB}\cdot\text{Hz}^{2/3}$ for a noise floor of $-140 \text{ dBm}/\text{Hz}$. When the optical carrier is partially suppressed, the SFDR is measured to be $91.5 \text{ dB}\cdot\text{Hz}^{2/3}$ for the same noise floor. As can be seen, an improvement in SFDR by 11 dB is achieved.

IV. CONCLUSION

A tunable single bandpass MPF with an improved SFDR using a DP-MZM and a PS-FBG has been proposed and demonstrated. The fundamental concept of the approach to achieve an improved SFDR was to partially suppress the optical carrier to increase the gain of the MPF, which was realized in the proposed approach by using the DP-MZM to generate an EPM signal with the power of the optical carrier controlled by the DC bias voltage to MZM1 to make the CSR be 0 dB while maintaining the optical power at the input of the PD unchanged by increasing the gain of the EDFA. In addition, by using the notch of the PS-FBG to remove one sideband of the EPM signal, PM-IM conversion was obtained, which led to an MPF with a single passband. An experiment was performed. A frequency-tunable single passband MPF with a frequency tunable range of 5.5 GHz and a constant bandwidth of 150 MHz during the tuning was demonstrated. The SFDR was improved by 11 dB. In the proposed MPF, the SFDR was increased by increasing the gain of the MPF. The IMD3 terms still exist. If we employ a technique to simultaneously increase the gain and to eliminate the IMD3 terms [13], [14], the SFDR can be further increased.

REFERENCES

- [1] R. A. Minasian, E. H. W. Chan, and X. Yi, "Microwave photonic signal processing," *Opt. Exp.*, vol. 21, no. 19, pp. 22918–22936, Sep. 2013.
- [2] J. Capmany, J. Mora, I. Gasulla, J. Sancho, J. Lloret, and S. Sales, "Microwave photonic signal processing," *J. Lightw. Technol.*, vol. 31, no. 4, pp. 571–586, Feb. 15, 2013.
- [3] J. Yao, "Microwave photonics," *J. Lightw. Technol.*, vol. 27, no. 3, pp. 314–335, Feb. 1, 2009.
- [4] J. Capmany, B. Ortega, and D. Pastor, "A tutorial on microwave photonic filters," *J. Lightw. Technol.*, vol. 24, no. 1, pp. 201–229, Jan. 2006.
- [5] J. Mora *et al.*, "Photonic microwave tunable single-bandpass filter based on a Mach-Zehnder interferometer," *J. Lightw. Technol.*, vol. 24, no. 7, pp. 2500–2509, Jul. 2006.
- [6] J. Palací, G. E. Villanueva, J. V. Galán, J. Martí, and B. Vidal, "Single bandpass photonic microwave filter based on a notch ring resonator," *IEEE Photon. Technol. Lett.*, vol. 22, no. 17, pp. 1276–1278, Sep. 1, 2010.
- [7] W. Li, M. Li, and J. Yao, "A narrow-passband and frequency-tunable microwave photonic filter based on phase-modulation to intensity-modulation conversion using a phase-shifted fiber Bragg grating," *IEEE Trans. Microw. Theory Techn.*, vol. 60, no. 5, pp. 1287–1296, May 2012.
- [8] W. Li and J. Yao, "A narrow-passband frequency-tunable microwave photonic filter with an improved dynamic range," in *Proc. OFC*, Anaheim, CA, USA, Mar. 2013, pp. 1–3, paper OTu2H.3.
- [9] T. Kawanishi, S. Sakamoto, and M. Izutsu, "High-speed control of lightwave amplitude, phase, and frequency by use of electrooptic effect," *IEEE J. Sel. Topics Quantum Electron.*, vol. 13, no. 1, pp. 79–91, Jan./Feb. 2007.
- [10] H. Chi, X. Zou, and J. Yao, "Analytical models for phase-modulation-based microwave photonic systems with phase modulation to intensity modulation conversion using a dispersive device," *J. Lightw. Technol.*, vol. 27, no. 5, pp. 511–521, Mar. 1, 2009.
- [11] V. J. Urick, K. J. Williams, and J. D. McKinney, *Fundamentals of Microwave Photonics*. Hoboken, NJ, USA: Wiley, 2015.
- [12] C. Lim, M. Attygalle, A. Nirmalathas, D. Novak, and R. Waterhouse, "Analysis of optical carrier-to-sideband ratio for improving transmission performance in fiber-radio links," *IEEE Trans. Microw. Theory Techn.*, vol. 54, no. 5, pp. 2181–2187, May 2006.
- [13] Y. Yan and J. Yao, "Photonic microwave bandpass filter with improved dynamic range," *Opt. Lett.*, vol. 33, no. 15, pp. 1756–1758, Aug. 2008.
- [14] X. Chen, W. Li, and J. Yao, "Microwave photonic link with improved dynamic range using a polarization modulator," *IEEE Photon. Technol. Lett.*, vol. 25, no. 14, pp. 1373–1376, Jul. 15, 2013.